


# Multi-Moment Formulation of Autoconversion Process and Radar Threshold Reflectivity

Yangang Liu[1], Peter Daum[1], Robert McGraw[1], Mark Miller[1], and Bart Geerts[2]

1- Brookhaven National Laboratory; 2- University of Wyoming

## 1. Introduction

Driver 1: Microphysics Parameterization — Driver 2: Radar Threshold Reflectivity

→ Autoconversion Process

→ Analytical Formulation & Observational Validation [by generalizing previous work (Liu & Daum 2004, Liu et al. 2004, 2005, 2006a, 2006b)]

## 2. General Formulation

For a bulk quantity $Y = \alpha\int r^\delta n(r)dr$,

autoconversion rate $P_Y = P_{Y\infty} T_Y$ (1)

$P_{Y\infty} \equiv$ Rate Function; $T_Y \equiv$ Threshold Function.

For $n(r) = \frac{q}{r_0^q} N r^{q-1}\exp\left[-\left(\frac{r}{r_0}\right)^q\right]$, Eq. (1) becomes

$$P_{Y\infty} = \alpha\left(\frac{3}{4\pi\rho_w}\right)^{(6+\delta)/3}\kappa\beta_6^6\beta_\delta^\delta N^{-\delta/3}L^{(6+\delta)/3}, \quad (2a)$$

$$T_Y = \gamma\left(\frac{6+q}{q}, x_{cq}\right)\gamma\left(\frac{\delta+q}{q}, x_{cq}\right), \quad (2b)$$

$$x_{cq} = \left(\frac{r_c}{r_0}\right)^q = \Gamma^{q/3}\left(\frac{3+q}{q}\right)x_c^{q/3}, \quad (2c)$$

$$x_c = \left(\frac{r_c}{r_3}\right)^3 = 9.7\times10^{-17}N^{3/2}L^{-2}, \quad (2d)$$

$$\beta_p^p = \Gamma\left(\frac{p+q}{q}\right)\Gamma^{-2}\left(\frac{3+q}{q}\right), \quad (2e)$$

$$\varepsilon = \left[\frac{2q\Gamma(2/q)}{\Gamma^2(1/q)} - 1\right]^{1/2} \approx q^{-1}, \quad (2f)$$

where $\kappa = 1.9 \times 10^{11}$ cm$^{-3}$s$^{-1}$ is a constant in the Long collection kernel, N droplet concentration, L liquid water content, $\varepsilon$ relative dispersion of the droplet size distribution, $\gamma$ the incomplete $\Gamma$ function, and $r_3$ the mean-volume radius.

## 3. Number Autoconversion Rate

### 3.1. General expressions

Setting $\alpha$ =1 and $\delta$ =0 in the above general expressions, we obtain the expressions for the number autoconversion rate:

$$P_{N\infty} = \left(\frac{3}{4\pi\rho_w}\right)^2\kappa\beta_6^6L^2 \quad (3a)$$

$$T_N = \gamma\left(\frac{6+q}{q}, x_{cq}\right)\gamma(1, x_{cq}) \quad (3b)$$

$$P_N = P_{N\infty}T_N$$

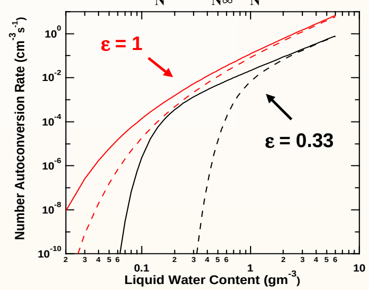


The dependency exhibits two distinct regimes: threshold function dominated regime and rate function dominated regime, and the difference between the two regimes increases with decreasing relative dispersion.

Figure 1 shows the dependence of the number autoconversion rate on liquid water content calculated from Eqs. (6a,b,c). The solid and dashed lines represent those for N = 50 cm-3 and N = 500 cm-3, respectively. The black and red colors represent those for $\varepsilon$ = 0.33 (q = 3) and $\varepsilon$ = 1(q =1), respectively.

### 3.2. Examination of existing schemes

Common assumption of existing multi-moment schemes:

$$P_N = \frac{3}{4\pi\rho_w r_*^3}P_L, \quad \text{with a constant } r_*$$

This assumption can be examined by combining our theoretical expressions for $P_N$ and $P_L$:

$$r_* = \left[\frac{\gamma\left(\frac{3+q}{q}, x_{cq}\right)}{\gamma(1, x_{cq})}\right]^{1/3} r_3 \quad (4)$$

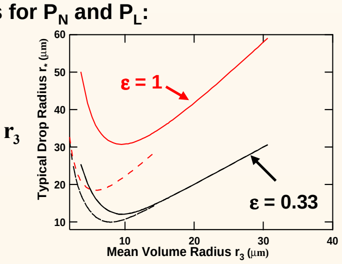


Figure 2 shows the dependence of $r_*$ on the mean-volume radius $r_3$ calculated from the theoretical expression for $r_*$. It is evident that the common assumption of a constant $r_*$ is incorrect, and the effects on modeling results need to be examined. The detail also depends on the droplet concentration and relative dispersion. The solid and dashed lines represent those for N = 50 cm$^{-3}$ and N = 500 cm$^{-3}$, respectively.

## 4. Radar Threshold Reflectivity

### 4.1. Theoretical expression and validation

For a typical size distribution with q = 3, Eq. (3b) becomes

$$T_N = \gamma(3, x_c)\gamma(1, x_c), \quad (5a)$$

$$x_c = 7.1\times10^{-16}N^{1/2}Z^{-1}, \quad (5b)$$

where Z is the radar reflectivity.

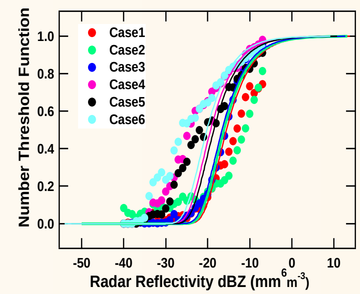


The measurements were made off the coast of N. California and Oregon using the PMS 2D-C probe and the U. Wyoming cloud radar onboard the U. of Wyoming King air aircraft.

Figure 3 shows the comparison of the theoretical threshold function to the observational results. The solid curves and dots are theoretical results and measurements, respectively. The colors of the theoretical curves correspond to those representing the observational results as given in the Figure Legend. Evidently, the theoretical expression compares favorably with observations, and discrepancies may be due to relative dispersion and measurement uncertainties.

### 4.2. Dependence of threshold reflectivity on droplet concentration

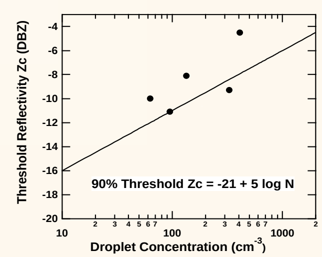


Figure 4 shows the dependence of the threshold reflectivity on the cloud droplet concentration. The black line and dots represent the theoretical and observational results, respectively. The threshold reflectivity can not be determined for Case 1 because there was very little drizzle.

## 5. Summary

- Multi-moment formulation for autoconversion process is derived theoretically.
- Number autoconversion rate is examined in detail, revealing deficiencies of existing schemes.
- Anylytical expressions for threshold reflectivity separating precipitating from nonprecipitating clouds are derived and compared to observations.
- Threshold reflectivity increases with increasing droplet concentration.